Published in final edited form as:

Circ Res. 2020 January 03; 126(1): 60–74. doi:10.1161/CIRCRESAHA.119.315180.

Glucose 6-Phosphate Accumulates via Phosphoglucose Isomerase Inhibition in Heart Muscle

Anja Karlstaedt[1], **Radhika Khanna**[2], **Manoj Thangam**[3], **Heinrich Taegtmeyer**[1]

[1]Department of Internal Medicine, Division of Cardiology, McGovern Medical School at The University of Texas Health Science Center at Houston, Houston, TX, USA

[2]Current affiliation: Ross University School of Medicine, Miramar, FL, USA

[3]Current affiliation: Department of Cardiology, Washington University School of Medicine in St. Louis, St. Louis, MO, USA

Abstract

Rationale: Metabolic and structural remodeling is a hallmark of heart failure. This remodeling involves activation of the mammalian target of rapamycin (mTOR) signaling pathway, but little is known on how intermediary metabolites are integrated as metabolic signals.

Objective: We investigated the metabolic control of cardiac glycolysis and explored the potential of glucose 6-phosphate (G6P) to regulate glycolytic flux and mTOR activation.

Methods and Results: We developed a kinetic model of cardiomyocyte carbohydrate metabolism, *CardioGlyco*, to study the metabolic control of myocardial glycolysis and G6P levels. Metabolic control analysis revealed that G6P concentration is dependent on phosphoglucose isomerase activity. Next, we integrated *ex vivo* tracer studies with mathematical simulations to test how changes in glucose supply and glycolytic flux affect mTOR activation. Nutrient deprivation promoted a tight coupling between glucose uptake and oxidation, G6P reduction, and increased protein-protein interaction between hexokinase II and mTOR. We validated the *in silico* modeling in cultured adult mouse ventricular cardiomyocytes by modulating phosphoglucose isomerase activity using erythrose 4-phosphate. Inhibition of glycolytic flux at the level of phosphoglucose isomerase caused G6P accumulation, which correlated with increased mTOR activation. Using click chemistry, we labeled newly synthesized proteins and confirmed that inhibition of phosphoglucose isomerase increases protein synthesis.

Conclusions: The reduction of phosphoglucose isomerase activity directly affects myocyte growth by regulating mTOR activation.

Graphical Abstract

Address correspondence to: Dr. Anja Karlstaedt, McGovern Medical School at The University of Texas Health Science Center at Houston, 6431 Fannin Street, MSB 1.404, Houston, TX, 77030, anja.karlstaedt@uth.tmc.edu.

DISCLOSURES.

None.

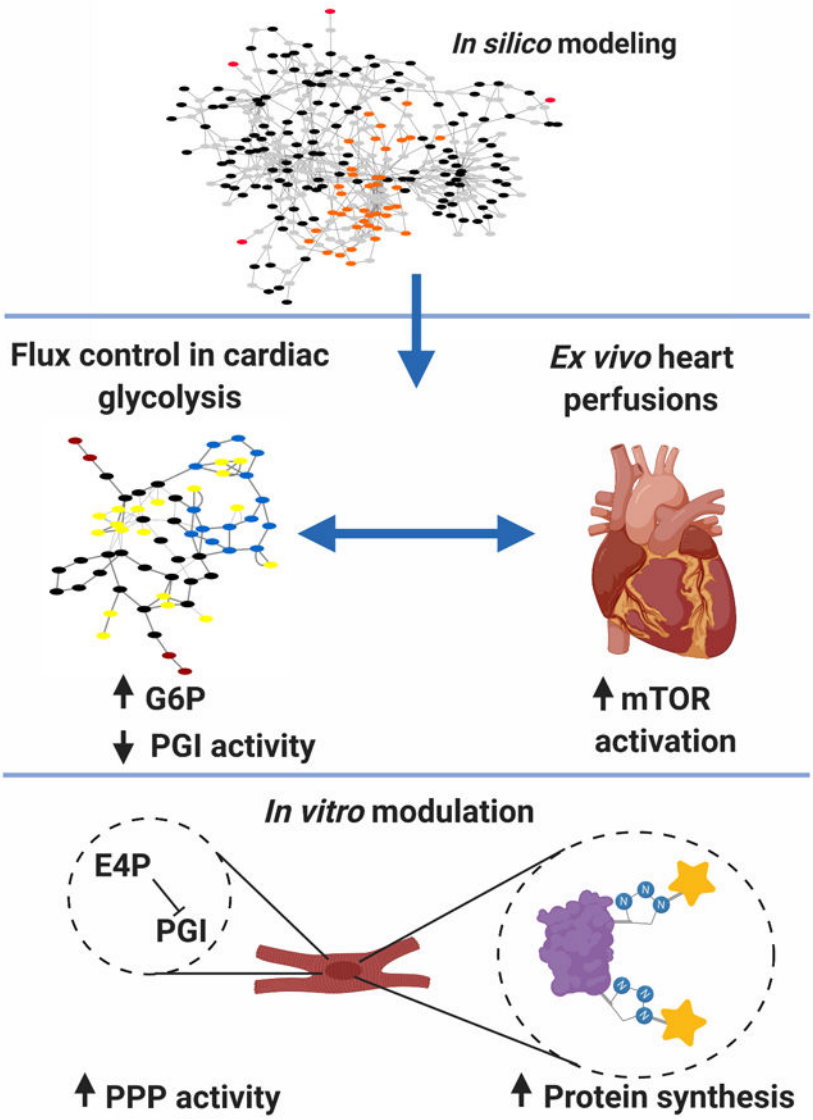

Keywords

Glycolysis; computer-based model; remodeling heart failure; cardiac metabolism; metabolic control analysis; Flux-balance analysis

Subject Terms:

Basic Science Research; Computational Biology; Heart Failure; Metabolism

INTRODUCTION

The heart balances its nutrient supply to meet the energy demands for coordinated contractile function. A host of adaptive responses to changes in the cellular environment sustains the pump function of the heart. When ATP demand exceeds the availability of

oxygen, the heart adapts by shifting from predominant oxidative phosphorylation (OxPhos) to glycolytic ATP provision. Alterations skewing this balance result in decreased cardiac function. Previous studies have already shown that cardiac hypertrophy is preceded by metabolic alterations, which promote changes in gene expression and cardiac remodeling[1-3]. Therefore, utilization of glucose can be a metabolic limitation for cardiac protein synthesis as well as renewal in response to stress. Numerous studies have described the link between the activation of signaling pathways and increased gene expression of proteins, which are part of metabolic pathways in the heart[4-7]. However, a direct link between changes in metabolite levels and the induction of structural remodeling or protein synthesis in the heart has not been elucidated. Thus, understanding the metabolic limitations of protein synthesis in the heart is critical to provide new insights into mechanisms of heart failure.

Deprivation of amino acids and glucose promotes structural changes through pathways regulated by the mammalian target of rapamycin complex 1 (mTORC1). The mTOR signal transduction pathway is a well-conserved central control pathway of growth in mammalian cells. Recent studies have revealed that inhibition of mTOR with rapamycin prevents cardiac hypertrophy, suggesting that mTOR and its downstream targets are involved in the pathogenesis of cardiac hypertrophy[8, 9]. Both cellular energy supply and demand regulate mTOR activity. We have previously shown in isolated working rat hearts that a mismatch between glucose uptake and oxidation, as well as ischemia-reperfusion, is associated with the accumulation of glucose 6-phosphate (G6P) and mTOR activation[10-12]. These findings raise the possibility that the dynamic of G6P concentration may support protein synthesis through activation of mTOR. Cell function is not only defined by its structure, but also defined by the concentration, activity, posttranslational modification state, or localization of molecule changes over time. G6P is uniquely placed at the intersection of three different metabolic pathways: glycolysis, glycogen synthesis, and the pentose phosphate pathway (PPP). Therefore, we sought to understand under which circumstances G6P is accumulating and how the production of G6P can be a metabolic driver for protein synthesis in some contexts.

To date, a number of groups have used mathematical modeling to study the dynamics of cardiac metabolism during nutrient deprivation and ischemia[13-18], including authors of this study[19]. Computational approaches provide a unique framework for studying interventions and potential strategies to improve cardiac function during stress. Here, we build upon these previous efforts to study how glycolytic control in cardiac metabolism can change G6P concentrations and how G6P may act as a metabolic signal during stress using both computational and experimental approaches. We first developed a simplified model of cardiomyocyte metabolism, *CardioGlyco*, that accounts for glycolysis, PPP, oxidation of pyruvate, and ATP turnover. Using metabolic control analysis (MCA) and constraint-based modeling (e.g., flux balance analysis, FBA), we show that G6P accumulation during hemodynamic and/or metabolic stress is controlled by phosphoglucose isomerase (PGI) activity. Next, we validated our mathematical modeling experimentally and study glucose supply differences in the isolated working rat heart using tracer experiments, thereby tracking flux and metabolite changes while evaluating cardiac function and mTOR activation. Lastly, we show that PGI inhibition in cultured adult mouse ventricular cardiomyocytes (AMVMs) results in increased mTOR activation and protein synthesis.

METHODS

The data that support the findings of this study are available from the corresponding author upon reasonable request.

A detailed description of materials and methods is available in the Supplemental Material.

Animals.

All animal experiments were conducted according to the Institutional Animal Care and Use Committee with guidelines issued by The University of Texas Health Science Center at Houston (see Supplemental Materials for details).

Isolated working rat heart perfusions.

Hearts were perfused by the method described earlier[20]. Further details are provided in the Supplemental Materials.

Determination of glucose oxidation rates with D[U-^{14}C]-glucose.

In working rat heart experiments, hearts were perfused with KH buffer containing D[U-^{14}C]-glucose (20 μCi/L, 9 dpm/nmol), and the coronary effluent was collected every minute. Rates of glucose oxidation were determined by the quantitative collection of $^{14}CO_2$ released in the coronary effluent. Further detailed information is given in the Supplemental Materials.

Isolation and culture of AMVMs.

AMVMs were isolated and cultured as described by O'Connell et al.[21]. Further detailed information is given in the Supplemental Materials.

Measurement of newly synthesized proteins using Click-IT chemistry, western blotting and immunoprecipitation.

Measurement of newly synthesized proteins was conducted using L-Azidohomoalanine (AHA) as described by Ma et al.[22]. Further detailed information is given in the Supplemental Materials.

Metabolic assays.

Metabolite concentrations and enzymatic activities were assessed colorimetrically using established enzymatic assays. Further detailed information on enzymatic assays, MCA, FBA, and rate equations for *CardioGlyco* are given in the Supplemental Materials.

Sample size calculations and statistical analysis.

Details are provided in the expanded Methods section in the Supplemental Materials.

CardioGlyco model.

The complete model is provided in the Systems Biology Markup Language (SBML) format on the EMBL BioModels platform (https://www.ebi.ac.uk/biomodels-main; MODEL1910170001).

RESULTS

Modeling myocardial glycolysis.

To investigate how G6P concentration is controlled, we first developed a model of myocardial glycolysis, *CardioGlyco*. This model is based on previously reported rate equations for glycolytic enzymes[23, 24]. We further curated the model to include both cardiac-specific rate equations[25-30] and initial metabolite concentrations[31, 32] (see Supplemental Materials and Online Tables I to XXI). The resulting kinetic model represented by the pathway shown in Figure 1A consists of two compartments, 18 reactions, and 20 metabolites, including redox cofactors (see Online Table III). In addition to evaluating lactate and pyruvate as products of glucose degradation, glycerol and glycogen were also considered in the system. Based on the model stoichiometry and physiological measurements of myocardial metabolite concentrations, we calculated steady-state flux rates as well as steady-state metabolite concentrations using COPASI (version 4.24.197 for windows)[33]. The model was validated with experimental data from previous studies on cardiac metabolism[31, 32]. Estimated steady-state concentrations are in good agreement with these reports (see Online Table XXI). *CardioGlyco* provides a theoretical framework to identify and design experimental strategies for the manipulation of myocardial glycolysis.

We conducted a metabolic control analysis (MCA)[34-36] (see Supplemental Methods for details) to understand the control structure of myocardial glycolysis and to identify which glycolytic enzyme influences G6P concentration. MCA distinguishes between the control of enzyme flux (flux control coefficient) and metabolite concentration (concentration control coefficient). Control coefficients describe how a flux or a metabolite concentration depends on a specific reaction rate in response to a perturbation of the entire system. Elasticity coefficients quantify reaction rate changes after perturbations of substrate concentrations or kinetic parameters (e.g., kinetic properties of an enzyme) [34-36]. The advantage of MCA is that it considers the system-wide effects of enzyme contributions rather than analyzing parts or single steps. Furthermore, the analysis helps to identify which quantities (e.g., enzymes, metabolites, fluxes) must be measured to determine the metabolic response of a biological system even to small perturbations. Thus, this approach differs from the concept of rate-limiting steps within metabolic pathways. Changes in the rate constant of an enzyme may be counterbalanced by other enzymes in the same pathway without affecting the overall flux. In other words, a glycolytic enzyme may have significant control on G6P concentration but not on the overall glycolysis flux.

Elasticities, flux control coefficients, and metabolite control coefficients were calculated using COPASI[33]. A positive concentration control coefficient indicates that the activation of the enzyme leads to an increase in the concentration of the metabolite, while a negative value indicates the opposite effect. As expected, G6P concentration is mainly determined by glucose uptake and phosphorylation (glucose transport and hexokinase activity) and phosphofructokinase (PFK) activity (Figure 1B). However, G6P concentration is also determined by PGI. Moreover, calculated elasticities for each enzyme in the model indicate that PGI activity is controlled by its effectors: F6P and G6P (Figure 1C). The model estimates a reduction of ATP hydrolysis when altering the glucose supply in simulations

from 5 to 2 mmol/L (Figure 1D). The participation of PGI in flux control results from the feedback inhibition of hexokinase (HK) by G6P. An inhibition of PGI would lead to an increase in G6P concentration, which diminishes glycolytic flux through inhibition of HK. Systematically decreasing PGI activity without changing parameters for any other enzymes leads to an increase in G6P and a corresponding decreased rate of the PGI reaction (Figure 1E). Our simulations indicate that both glucose supply and PGI activity, in addition to HK and PFK, play an important role in the regulation of glycolysis.

Cardiac performance as a function of glucose supply.

We conducted working rat heart perfusions and integrated the metabolic data into mathematical network modeling to test whether acute changes in glucose supply activate mTOR and whether this activation is promoted by an impairment of glycolysis. Wild-type (WT) Sprague-Dawley rat hearts were perfused *ex vivo* at near physiologic (5 mmol/L) and sub-physiologic (3 and 2 mmol/L) glucose concentrations (n = 4 rats/ group). Endogenous substrates were depleted during the initial 20 min of the perfusion and replenished at physiologic glucose concentrations (5 mmol/L) as described before by Goodwin et al[37, 38]. This approach ensured that variations in the intracellular glycogen storages between animals did not influence the effect of decreased glucose supply on cardiac metabolism and function. In the subsequent 30 min, we observed a decreased contractile function in hearts perfused with 2 mmol/L glucose, before and after an imposed increase in cardiac work (Figure 2A). Further, during stimulation with epinephrine the inotropic response was significantly lower with 2 mmol/L glucose supply compared to 3 or 5 mmol/L (P-value <0.001). We used uniformly labeled glucose (D[U-^{14}C]-glucose) to compare glucose oxidation rates between groups[37]. The $^{14}CO_2$ production from [U-^{14}C]-glucose inversely correlated with the supplied glucose concentration from the perfusate during prolonged stimulation (Figure 2B), while myocardial oxygen consumption (MVO_2) correlated with glucose supply (Figure 2C). Tissue analyses of hearts freeze-clamped at the end of the perfusion protocol confirmed that the tissue ATP content was decreased, and AMP content was increased in a glucose concentration-dependent manner (Figure 2D). The results indicate that our experimental model imposed metabolic stress on the heart, causing a discrepancy between energy substrate supply and demand.

To assess cardiac metabolic changes in response to reduced glucose supply, we determined the activities of HK, PFK, G6PDH (glucose 6-phosphate dehydrogenase), LDH, MDH (malate dehydrogenase), GLDH (glutamate dehydrogenase), and PK (pyruvate kinase) from perfused rat hearts (Figure 3A and B). HK activity was unchanged between the experimental groups (Figure 3A). The K_m value of HK is 0.2 mmol/L; thus, HK has a high affinity for glucose and operates at maximal velocity even at sub-physiologic glucose concentrations. In contrast, PFK and PK activity correlated in an inverse relationship with glucose supply, while LDH, GLDH, MDH, and G6PDH activity correlated with glucose supply (Figure 3A and B). These results indicate that glucose-derived pyruvate is entering the Krebs cycle rather than being converted to lactate (as depicted in schematic Figure 3C), which suggests a tight coupling between glucose uptake and oxidation at sub-physiological glucose supply. In other words, in situations of sparse nutrient supply, ATP is provided through oxidative metabolism of glucose in the heart.

mTOR activation and cardiac metabolic adaptation.

To assess the impact of exogenous glucose on mTOR activation, we next determined the expression of mTOR and upstream regulators (AMPK [AMP kinase] and TSC2 [tuberin sclerosis complex 2]). Sub-physiologic glucose supply (3 and 2 mmol/L) was associated with decreased mTOR phosphorylation and activation (Figure 4A). Correspondingly, the level of phosphorylation and activation of AMPK (Figure 4A) and TSC2 (Figure 4B) increased. Previously, we have shown that increased workload is associated with the accumulation of the glycolytic intermediate G6P and increased mTOR phosphorylation and activation[39]. Like in these previous observations, we found that G6P concentration in perfused hearts correlated with mTOR phosphorylation (Figure 4C). Previous reports indicate that HK II directly inhibits mTORC1 activity in response to glucose deprivation[40, 41]. Therefore, we tested whether HK II and mTORC1 interact during our experimental conditions using immunoprecipitation studies. We immunoprecipitated mTOR from perfused and freeze-clamped hearts followed by Western blotting for HK II. Consistent with previous studies, we observed an increased protein-protein interaction of mTOR and HK II with decreasing glucose concentrations in the perfusion buffer (Figure 4D), suggesting that HK II associates with mTORC1 in response to glucose deprivation. Our results show that a simultaneous increase in cardiac workload and sub-physiologic glucose supply results in G6P reduction and impaired ATP provision (reduced ATP/AMP ratio, see Figure 2C). This, in turn, stimulates AMPK and TSC2 phosphorylation and activation.

In silico modeling links PGI activity with PPP flux.

CardioGlyco allows the mathematical evaluation of glycolysis and to test the influence of enzymatic parameters on metabolite concentration and flux. However, the model is limited by the number of included reactions. To test whether pathways other than glycolysis are involved in regulating the concentration of G6P in the metabolically stressed heart, we estimated flux distributions using the genome-scale model of mammalian cardiac metabolism, *CardioNet*[19]. To calculate flux distributions, we used rates for glucose oxidation and myocardial oxygen consumption determined during the isolated working rat heart perfusions (see Figure 2B and C). We also included enzyme activity changes for HK, MDH, LDH, PK, and GLDH measured in tissue samples from perfused hearts freeze-clamped at the end of the perfusion protocol (see Supplemental Methods for details). Next, we compared estimated flux rates between experimental groups to identify which metabolic reactions change in response to different glucose supply (Figure 5A). We found significant differences for the following enzymes or processes: citrate synthase (CS), PGI, isocitrate dehydrogenases (IDHs) 1, 2, and 3, fatty acid oxidation (FAOX), and OxPhos. We identified four main clusters that were clearly separated by pathways and energy providing substrates. Reactions for (1) FAOX and OxPhos, (2) glycolysis and Krebs cycle, (3) IDH 1, and (4) MDH reactions clearly clustered separately. These reactions/pathways reflect the oxidation of both glucose and fatty acids (e.g., palmitate and oleate), demonstrating the increased reliance on endogenous pools (e.g., lipids) with low glucose supply.

Using FBA, we assessed theoretically whether alterations in the activities of these enzymes/processes affect G6P synthesis. FBA simulations revealed that decreasing the activity of PGI promotes redirection of carbons into the PPP (Figure 5B). The oxidative and non-oxidative

branch of the PPP bypassed an inhibition of PGI and provided F6P as well as glycerol 3-phosphate (G3P) to ensure flux through the lower part of the glycolysis. Due to the limitations of FBA, we conducted additional kinetic modeling using an expanded version of *CardioGlyco*, which contains the PPP (Figure 6A) (see Supplemental Materials and Online Table XXII **to** XXXI for rate equations and initial metabolite concentrations). The expanded version of *CardioGlyco* correctly estimates internal metabolite concentrations and flux rates as a function of time (see Online Figure I). The model predicts flux through the PPP when the extracellular glucose concentration is set to 5.5 mmol/L. However, the flux is relatively low compared to HK, PGI, and PFK. As depicted in Online Figure II, increasing the activity of glucose transport (GLUT) and LDH increases the amount of G6P. Conversely, decreasing the activity of PGI and PFK will decrease the amount of G6P. Previous studies have shown that PGI deficiency results in a reduction of PGI activity to 20% *in vivo*[42]. Using *CardioGlyco*, we simulated a PGI inhibition and predicted metabolite as well as flux rate changes as a function of time. As depicted in Figure 6 B and C, G6P concentration increases while PFK and PGI flux decrease compared to normal conditions (see Online Figure I). Correspondingly, G6PDH increases in response to PGI inhibition during the simulations indicating that G6P is redirected into the PPP. Therefore, we reasoned that PGI is a crucial metabolic checkpoint for glucose uptake and glucose oxidation.

PGI inhibition increases G6P levels and increases G6PDH activity.

To test our mathematical predictions, we used a small-molecule inhibitor, erythrose 4-phosphate (E4P), to modulate PGI activity in isolated adult mouse ventricular cardiomyocytes (AMVMs) (see Methods for details). PGI also has a non-metabolic function and can be secreted as a cytokine even when its enzymatic activity is impaired[43]. Therefore, we decided to use E4P, an active-site inhibitor of PGI, which allowed the modification of PGI activity without affecting protein expression and study the metabolic impact of flux redirection on protein synthesis. AMVMs were cultured in the presence of glucose (5.5 mmol/L) and glutamine (2 mmol/L) (see Methods for details). We replaced the culture media after 24 h and added the PGI inhibitor E4P (3 μM) or vehicle (PBS) to the cultured AMVMs for another 24 h. Our experimental conditions facilitate E4P uptake across a concentration gradient. *In vitro* E4P treatment reduced PGI activity (Figure 7A) and increased G6PDH activity (Figure 7B). PFK activity was not changed under the experimental conditions (Figure 7C). PGI inhibition was associated with a 2-fold increased G6P concentration (Figure 7D). Our data indicate that reduced glucose utilization promotes G6P accumulation and leads to a redirection of carbons into the PPP as predicted by *in silico* simulations.

PGI inhibition promotes mTOR activation and increases protein synthesis.

To further assess whether inhibition of PGI activates mTOR and protein synthesis, we treated AMVMs with PBS, E4P (3 μmol/L), or rapamycin (20 nmol/L) alone and in combination. Rapamycin binds mTOR allosterically and inhibits mTORC1 activity. As expected, we observed that mTOR phosphorylation decreased with increasing rapamycin concentration (Figure 8A). Inhibition of PGI with E4P did not affect its protein expression, while mTORC1 inhibition with rapamycin decreased PGI expression (Figure 8B).

Correspondingly, we observed increased phosphorylation and activation of mTOR with PGI inhibition, while rapamycin had the opposite effect (Figure 8C).

Next, we determined whether PGI inhibition changes the amount of newly synthesized proteins using the synthetic methionine homolog L-azidohomoalanine (AHA; 50 μg/ mL for two h) and click chemistry (see Methods for details). AMVMs were grown as described above with either vehicle (PBS, control) or E4P for 24 h. At the end of the treatment, we added to some cells 2-deoxyglucose (2DG; 25 mmol/L) or cycloheximide (CHX; 10 μg/ mL) as controls. Measurements of AHA labeling in AMVMs indicated that protein synthesis rates were increased under E4P treatments (Figure 8D). E4P-treated cardiomyocytes showed higher AHA incorporation compared to untreated cells. We detected higher AHA incorporation even when cells were treated with 2DG and CHX. Our findings show that PGI inhibition increases G6P level and G6PDH activity, which is associated with an increase in protein synthesis rate (Figure 8E).

DISCUSSION

Cardiac metabolism rapidly adapts to various forms of stress (e.g., hemodynamic, neurohumoral, or metabolic stress) to ensure energy provision and uninterrupted contractile function. With a mismatch between energy supply and demand, the heart switches its nutrient utilization from predominate oxidation of fatty acids towards oxidation of glucose. Therefore, the utilization of glucose can be a metabolic determinant of cardiac protein synthesis and renewal in response to stress. We demonstrated that PGI inhibition promotes G6P accumulation and supports protein synthesis in AMVMs. These concepts are based on the following findings: (1) mathematical modeling using MCA and FBA showed that PGI activity exhibits control on G6P, (2) glucose utilization and energy demand regulate mTOR activation, (3) kinetic modeling predicts a direction of G6P into the PPP upon inhibition of PGI, and (4) E4P-mediated PGI inhibition is associated with increased protein synthesis in AMVMs.

Mathematical modeling reveals PGI as a flux-controlling step.

Mathematical modeling of biological systems allows the determination of flux rate and metabolite concentration changes in response to stress on a systems level. This theoretic approach can be used to identify potential regulators and metabolic targets. Genome-scale metabolic networks like *CardioNet* estimate flux distributions using constrained-based modeling once an equilibrium or steady-state has been reached. However, dynamic simulations are necessary to understand the transient state of cardiac metabolism during acute stress conditions (e.g., ischemia-reperfusion, exercise, shock). A major challenge in modeling cardiac metabolism arises from limited information of enzyme kinetics in pathways other than glycolysis. These limitations currently prevent an accurate representation of cardiac metabolism using rate equations on a genome-scale. Additionally, MCA quantitatively determines the control of enzymes on a pathway rather than using more intuitive concepts of “key enzymes” or “rate-limiting steps”. In fact, flux control is shared by multiple reactions in a pathway and may not be limited to a single enzyme. Kinetic models of cardiac metabolism, e.g., *CardioGlyco*, improve our understanding of metabolic reactions

and provide a framework to design experimental studies. Here, we established a new framework for the comprehensive analysis of cardiac metabolic response to nutrient stress *in silico*. The model, *CardioGlyco*, is a starting point to develop a comprehensive kinetic model of mammalian cardiac metabolism. Using MCA, we determined that PGI exerts control on G6P concentration and flux through glycolysis and the PPP (Figure 8E).

Enzyme inhibition as a model for inborn errors of metabolism.

PGI deficiency is a rare inherited metabolic defect or "inborn error of metabolism" (IEM) that results in a less stable protein homodimer impairing its enzymatic activity and interfering with energy substrate metabolism as well as cell differentiation in different cell types, e.g., erythrocytes, neurons, and hematopoietic stem cells. Patients often present with hemolytic anemia and neurological symptoms. PGI is uniquely positioned at the intersection between three irreversible steps: (1) the phosphorylation of F6P by PFK, (2) the hydrolyzation of G6P by G6P dehydrogenase (G6PDH), and (3) the hexosamine synthetic pathway. Therefore, any perturbances in PGI activity affect both glycolytic and PPP fluxes. PGI deficiency as an IEM may help us to understand in a broader context how cardiomyocytes respond to inhibition of PGI activity and flux[44-46]. Baughan *et al.* showed that the PPP in PGI-deficient erythrocytes was activated at maximum levels, even in the absence of oxidative stress[42]. Furthermore, glucose utilization was not efficient due to decreased isomerization of G6P and F6P. Correspondingly, we found that PGI inhibition increased G6PDH activity, suggesting an increased flux through the PPP. Further, our data indicate that increasing PPP may induce protein synthesis through activation of mTORC1.

Glucose utilization regulates mTOR activation.

How metabolic pathways support cardiac remodeling, and contractile function has been extensively studied in response to myocardial infarction or chronic pressure overload[5-7, 47]. These findings support the hypothesis that glycolytic intermediates modulate mTOR activity in addition to known regulators of the system (e.g., amino acids). Our modeling predicted that changing the extracellular glucose concentration from 5 to 2 mmol/L reduces ATP provision. We show that the contribution of OxPhos decreases at sub-physiologic glucose supply, as evidenced by a mismatch between $^{14}CO_2$ production and oxygen consumption. This mismatch is likely caused by insufficient glucose supply and/or by changes in the perfusion pressure after the acute stimulation phase. Oxygen delivery and coronary flow depend on perfusion pressure in the working heart preparation. To prevent this "demand ischemia", we designed our perfusion experiments using a combined intervention with epinephrine stimulation and increased afterload by 40% (aortic column)[37, 48]. We reasoned that the observed changes in oxygen consumption and glucose oxidation are due to metabolic changes. Decarboxylation of glucose occurs in the Krebs cycle and the oxidative branch of the PPP. We found that G6PDH and LDH activities are decreased while PFK and PK activities increased at sub-physiologic glucose supply. These data indicate that exogenous glucose is almost exclusively channeled into the Krebs cycle when glucose supply is low. However, even with a tight coupling between glucose uptake and oxidation, the amount of glucose oxidation and oxygen consumption does not yield enough ATP provision, as reflected in a reduction in hydraulic power.

Consequently, we concluded that the heart is increasingly utilizing endogenous carbon sources, e.g., glycogen, when glucose supply is low. Metabolic adaptation in the heart is characterized by the ability to maintain high-energy phosphates (e.g., ATP) and preserve endogenous substrates (e.g., glycogen). Our previous studies showed that high fat and lactate attenuate net glycogenolysis during acute and prolonged adrenergic stimulation[37, 48-50]. Our data indicate that at sub-physiologic glucose supply, the heart draws on its glycogen reserve to maintain contractile function.

G6P is redirected into the PPP upon PGI inhibition.

Sustained inhibition of PGI induces the accumulation of G6P, leading to increased mTOR phosphorylation and activation. Based on our *in silico* modeling, upon PGI inhibition, cardiac metabolism adapts by increasing G6P concentration and redirects glycolytic intermediates into the PPP. In fact, *in vitro* experiments showed increased activity of G6PDH, the rate-limiting step of the PPP, in response to PGI inhibition. These findings suggest that upon metabolic stress, carbon flux is redirected from glycolysis into the PPP to potentially support biosynthetic processes, which, in turn, may support adaptation. Enhanced glycolysis in proliferating cells (e.g., cancer cells) provides an advantage for growth by maintaining macromolecular precursors for some amino acids beyond providing ATP, and through the regeneration of reducing equivalents for metabolic reactions (e.g., NADPH and NADH). NADPH provides reducing equivalents to maintain the cellular redox state and is primarily regenerated in the oxidative portion of the PPP through reactions of the G6PDH and 6-phosphogluconolactonate dehydrogenase. Other sources of NADPH have been suggested in human glioma cells through the decarboxylation of glutamine by MDH[51]. Glutamine-derived lactate can generate up to one molecule of NADPH in glioma cells if glutamine is metabolized to malate, which, in turn, is converted to pyruvate through MDH. Additional studies, however, are required to determine whether these alternative NADPH-generating pathways are also present and active in cardiomyocytes. High NADPH is a driving force for fatty acid synthesis, helps to maintain reduced glutathione pools, and has been linked to mTOR activation[52, 53]. In fact, the expression of metabolic genes involved in the PPP is partially controlled through mTORC1-dependent activation of sterol responsive element binding protein (SREBP) transcription factors[54]. Conversely, the mTOR inhibitor rapamycin has been shown to reduce NADPH regeneration and limit cell growth[55]. Our findings provide further evidence that glycolytic intermediates modulate mTOR activity in addition to providing macromolecule precursors.

Study limitations.

There are limitations to this study. First, mathematical modeling of biological systems is biased towards known enzymes and metabolites. Both *CardioNet* and *CardioGlyco* do not account for electrolyte changes. Nevertheless, in the scope of our study, both models have proven to be valuable to guide experimental design and targeted analysis. Second, modeling of the PPP is limited using *CardioGlyco* due to the lack of kinetic parameters and internal metabolite concentrations from the mammalian heart. Currently, the model includes kinetic parameters that were determined in mammalian heart and yeast. Third, uniformly labeled glucose ([U-^{14}C]glucose) can be used to determine the rate of glucose oxidation from exogenous glucose in the Krebs cycle and in the oxidative branch of the PPP. However, we

cannot conclude which pathway is responsible for glucose oxidation from measuring $^{14}CO_2$ alone. Additional tracer experiments are required to determine the contribution of endogenous glucose (e.g., from glycogen). Thus, we complemented our tracer experiments by measuring metabolite concentrations and enzymatic activities.

Conclusions.

The predictive value of *in silico* modeling provided us with a framework to analyze which enzymes exert control on G6P concentration and to design experiments using targeted modulation of enzyme activities. The metabolic reprogramming of cardiomyocytes does not occur in isolation but integrates other signaling events in response to physiologic and pathologic stress. Looking ahead to expand our understanding of cardiac remodeling, we are interested in studying the role of mTOR and TSC2 in regulating metabolism and structural remodeling in the heart. Together with genetic and mathematical approaches, we are gaining important insights into the relationship between glycolysis and protein turnover in the heart.

Supplementary Material

Refer to Web version on PubMed Central for supplementary material.

ACKNOWLEDGMENTS.

We thank all members of the Taegtmeyer laboratory for their valuable discussions. We thank Jiries Ganim and Hanna Shanar for helping with collecting and evaluating kinetic parameters for mathematical simulations.

SOURCES OF FUNDING.

The work was supported by the Friede Springer Herz Stiftung, Germany (to A.K.), the Roderick MacDonald Research Fund (15RDM005 to A.K.), the American Heart Association (17POST33660221 to A.K.) and NIH (R01-HL-061483 to H.T. and K99-HL-141702 to A.K.).

Nonstandard Abbreviations And Acronyms:

AHA	L-azidohomoalanine
AMPK	AMP Kinase
AMVM	adult mouse ventricular cardiomyocyte
CHX	cycloheximide
CS	citrate synthase
E4P	erythrose 4-phosphate
2DG	2-deoxyglucose
FAOX	fatty acid oxidation
FBA	flux balance analysis
F6P	fructose 6-phosphate
G6P	glucose 6-phosphate

G6PDH	glucose 6-phosphate dehydrogenase
GAPDH	glucose 3-phosphate dehydrogenase
GLDH	glutamate dehydrogenase
HK	hexokinase
IDH	isocitrate dehydrogenase
IEM	inborn errors of metabolism
KH	Krebs Henseleit
MCA	metabolic control analysis
MDH	malate dehydrogenase
mTORC1	mammalian target of rapamycin complex 1
PGI	phosphoglucose isomerase
PEP	phosphoenolpyruvate
PFK	phosphofructokinase
PK	pyruvate kinase
PPP	pentose phosphate pathway
OxPhos	oxidative phosphorylation
TSC2	tuberin sclerosis complex 2
WT	wild type

REFERENCES

1. Taegtmeyer H, Overturf ML. Effects of moderate hypertension on cardiac function and metabolism in the rabbit. Hypertension. 1988;11:416–426 [PubMed: 3366475]
2. Young ME, Laws FA, Goodwin GW, Taegtmeyer H. Reactivation of peroxisome proliferator-activated receptor alpha is associated with contractile dysfunction in hypertrophied rat heart. J Biol Chem. 2001;276:44390–44395 [PubMed: 11574533]
3. Young ME, Yan J, Razeghi P, Cooksey RC, Guthrie PH, Stepkowski SM, McClain DA, Tian R, Taegtmeyer H. Proposed regulation of gene expression by glucose in rodent heart. Gene Regul Syst Bio. 2007;1:251–262
4. Shao D, Villet O, Zhang Z, Choi SW, Yan J, Ritterhoff J, Gu H, Djukovic D, Christodoulou D, Kolwicz SC Jr., Raftery D, Tian R. Glucose promotes cell growth by suppressing branched-chain amino acid degradation. Nat Commun. 2018;9:2935 [PubMed: 30050148]
5. Das A, Durrant D, Koka S, Salloum FN, Xi L, Kukreja RC. Mammalian target of rapamycin (mtor) inhibition with rapamycin improves cardiac function in type 2 diabetic mice: Potential role of attenuated oxidative stress and altered contractile protein expression. J Biol Chem. 2014;289:4145–4160 [PubMed: 24371138]
6. Volkers M, Doroudgar S, Nguyen N, Konstandin MH, Quijada P, Din S, Ornelas L, Thuerauf DJ, Gude N, Friedrich K, Herzig S, Glembotski CC, Sussman MA. Pras40 prevents development of

diabetic cardiomyopathy and improves hepatic insulin sensitivity in obesity. EMBO Mol Med. 2014;6:57–65 [PubMed: 24408966]

7. Aoyagi T, Kusakari Y, Xiao CY, Inouye BT, Takahashi M, Scherrer-Crosbie M, Rosenzweig A, Hara K, Matsui T. Cardiac mtor protects the heart against ischemia-reperfusion injury. Am J Physiol Heart Circ Physiol. 2012;303:H75–85 [PubMed: 22561297]
8. Heineke J, Molkentin JD. Regulation of cardiac hypertrophy by intracellular signalling pathways. Nat Rev Mol Cell Biol. 2006;7:589–600 [PubMed: 16936699]
9. Shioi T, McMullen JR, Tarnavski O, Converso K, Sherwood MC, Manning WJ, Izumo S. Rapamycin attenuates load-induced cardiac hypertrophy in mice. Circulation. 2003;107:1664–1670 [PubMed: 12668503]
10. Foster DB, Liu T, Rucker J, O'Meally RN, Devine LR, Cole RN, O'Rourke B. The cardiac acetyl-lysine proteome. PLoS One. 2013;8:e67513 [PubMed: 23844019]
11. Sharma S, Guthrie PH, Chan SS, Haq S, Taegtmeyer H. Glucose phosphorylation is required for insulin-dependent mtor signalling in the heart. Cardiovasc Res. 2007;76:71–80 [PubMed: 17553476]
12. Taegtmeyer H, Roberts AF, Raine AE. Energy metabolism in reperfused heart muscle: Metabolic correlates to return of function. J Am Coll Cardiol. 1985;6:864–870 [PubMed: 4031301]
13. Kashiwaya Y, Sato K, Tsuchiya N, Thomas S, Fell DA, Veech RL, Passonneau JV. Control of glucose utilization in working perfused rat heart. J Biol Chem. 1994;269:25502–25514 [PubMed: 7929251]
14. McDougal AD, Dewey CF, Jr. Modeling oxygen requirements in ischemic cardiomyocytes. J Biol Chem. 2017;292:11760–11776 [PubMed: 28487363]
15. Wu F, Zhang EY, Zhang J, Bache RJ, Beard DA. Phosphate metabolite concentrations and atp hydrolysis potential in normal and ischaemic hearts. J Physiol. 2008;586:4193–4208 [PubMed: 18617566]
16. Ch'en FF, Vaughan-Jones RD, Clarke K, Noble D. Modelling myocardial ischaemia and reperfusion. Prog Biophys Mol Biol. 1998;69:515–538 [PubMed: 9785954]
17. Tepp K, Timohhina N, Chekulayev V, Shevchuk I, Kaambre T, Saks V. Metabolic control analysis of integrated energy metabolism in permeabilized cardiomyocytes - experimental study. Acta Biochim Pol. 2010;57:421–430 [PubMed: 21170421]
18. Cortassa S, Aon MA, O'Rourke B, Jacques R, Tseng HJ, Marban E, Winslow RL. A computational model integrating electrophysiology, contraction, and mitochondrial bioenergetics in the ventricular myocyte. Biophys J. 2006;91:1564–1589 [PubMed: 16679365]
19. Karlstädt A, Fliegner D, Kararigas G, Ruderisch HS, Regitz-Zagrosek V, Holzhütter H-G. Cardionet: A human metabolic network suited for the study of cardiomyocyte metabolism. BMC Syst Biol. 2012;6:114 [PubMed: 22929619]
20. Taegtmeyer H, Hems R, Krebs HA. Utilization of energy-providing substrates in the isolated working rat heart. Biochem J. 1980;186:701–711 [PubMed: 6994712]
21. O'Connell TD, Rodrigo MC, Simpson PC. Isolation and culture of adult mouse cardiac myocytes. Methods Mol Biol. 2007;357:271–296 [PubMed: 17172694]
22. Ma Y, McClatchy DB, Barkallah S, Wood WW, Yates JR, 3rd. Quantitative analysis of newly synthesized proteins. Nat Protoc. 2018;13:1744–1762 [PubMed: 30038347]
23. Teusink B, Westerhoff HV. 'Slave' metabolites and enzymes. A rapid way of delineating metabolic control. Eur J Biochem. 2000;267:1889–1893 [PubMed: 10727927]
24. Teusink B, Passarge J, Reijenga CA, Esgalhado E, van der Weijden CC, Schepper M, Walsh MC, Bakker BM, van Dam K, Westerhoff HV, Snoep JL. Can yeast glycolysis be understood in terms of in vitro kinetics of the constituent enzymes? Testing biochemistry. Eur J Biochem. 2000;267:5313–5329 [PubMed: 10951190]
25. Cheung JY, Conover C, Regen DM, Whitfield CF, Morgan HE. Effect of insulin on kinetics of sugar transport in heart muscle. Am J Physiol. 1978;234:E70–78 [PubMed: 623253]
26. Grossbard L, Schimke RT. Multiple hexokinases of rat tissues. Purification and comparison of soluble forms. J Biol Chem. 1966;241:3546–3560 [PubMed: 5919684]

27. Knight RJ, Kofoed KF, Schelbert HR, Buxton DB. Inhibition of glyceraldehyde-3-phosphate dehydrogenase in post-ischaemic myocardium. Cardiovasc Res. 1996;32:1016–1023 [PubMed: 9015404]
28. Evans RK, Scoville CR, Ito MA, Mello RP. Upper body fatiguing exercise and shooting performance. Mil Med. 2003;168:451–456 [PubMed: 12834134]
29. Borgmann U, Moon TW, Laidler KJ. Molecular kinetics of beef heart lactate dehydrogenase. Biochemistry. 1974;13:5152–5158 [PubMed: 4373032]
30. Nascimben L, Ingwall JS, Lorell BH, Pinz I, Schultz V, Tornheim K, Tian R. Mechanisms for increased glycolysis in the hypertrophied rat heart. Hypertension. 2004;44:662–667 [PubMed: 15466668]
31. Bround MJ, Wambolt R, Luciani DS, Kulpa JE, Rodrigues B, Brownsey RW, Allard MF, Johnson JD. Cardiomyocyte atp production, metabolic flexibility, and survival require calcium flux through cardiac ryanodine receptors in vivo. J Biol Chem. 2013;288:18975–18986 [PubMed: 23678000]
32. Donohoe JA, Rosenfeldt FL, Munsch CM, Williams JF. The effect of orotic acid treatment on the energy and carbohydrate metabolism of the hypertrophying rat heart. Int J Biochem. 1993;25:163–182 [PubMed: 8444313]
33. Hoops S, Sahle S, Gauges R, Lee C, Pahle J, Simus N, Singhal M, Xu L, Mendes P, Kummer U. Copasi--a complex pathway simulator. Bioinformatics. 2006;22:3067–3074 [PubMed: 17032683]
34. Heinrich R, Rapoport TA. A linear steady-state treatment of enzymatic chains. Critique of the crossover theorem and a general procedure to identify interaction sites with an effector. Eur J Biochem. 1974;42:97–105 [PubMed: 4830199]
35. Heinrich R, Rapoport TA. A linear steady-state treatment of enzymatic chains. General properties, control and effector strength. Eur J Biochem. 1974;42:89–95 [PubMed: 4830198]
36. Rapoport TA, Heinrich R, Jacobasch G, Rapoport S. A linear steady-state treatment of enzymatic chains. A mathematical model of glycolysis of human erythrocytes. Eur J Biochem. 1974;42:107–120 [PubMed: 4364392]
37. Goodwin GW, Ahmad F, Doenst T, Taegtmeyer H. Energy provision from glycogen, glucose, and fatty acids on adrenergic stimulation of isolated working rat hearts. Am J Physiol. 1998;274:H1239–H1247 [PubMed: 9575927]
38. Goodwin GW, Taylor CS, Taegtmeyer H. Regulation of energy metabolism of the heart during acute increase in heart work. J Biol Chem. 1998;273:29530–29539 [PubMed: 9792661]
39. Sen S, Kundu BK, Wu HC, Hashmi SS, Guthrie P, Locke LW, Roy RJ, Matherne GP, Berr SS, Terwelp M, Scott B, Carranza S, Frazier OH, Glover DK, Dillmann WH, Gambello MJ, Entman ML, Taegtmeyer H. Glucose regulation of load-induced mtor signaling and er stress in mammalian heart. J Am Heart Assoc. 2013;2:e004796 [PubMed: 23686371]
40. Roberts DJ, Miyamoto S. Hexokinase ii integrates energy metabolism and cellular protection: Akting on mitochondria and torcing to autophagy. Cell Death Differ. 2015;22:248–257 [PubMed: 25323588]
41. Roberts DJ, Tan-Sah VP, Ding EY, Smith JM, Miyamoto S. Hexokinase-ii positively regulates glucose starvation-induced autophagy through torc1 inhibition. Mol Cell. 2014;53:521–533 [PubMed: 24462113]
42. Baughan MA, Valentine WN, Paglia DE, Ways PO, Simons ER, DeMarsh QB. Hereditary hemolytic anemia associated with glucosephosphate isomerase (gpi) deficiency--a new enzyme defect of human erythrocytes. Blood. 1968;32:236–249 [PubMed: 5672849]
43. Tsutsumi S, Gupta SK, Hogan V, Tanaka N, Nakamura KT, Nabi IR, Raz A. The enzymatic activity of phosphoglucose isomerase is not required for its cytokine function. FEBS Lett. 2003;534:49–53 [PubMed: 12527360]
44. Fujii H, Kanno H, Hirono A, Miwa S. Hematologically important mutations: Molecular abnormalities of glucose phosphate isomerase deficiency. Blood Cells Mol Dis. 1996;22:96–97 [PubMed: 8931949]
45. Kanno H, Fujii H, Hirono A, Ishida Y, Ohga S, Fukumoto Y, Matsuzawa K, Ogawa S, Miwa S. Molecular analysis of glucose phosphate isomerase deficiency associated with hereditary hemolytic anemia. Blood. 1996;88:2321–2325 [PubMed: 8822954]

46. Kanno H, Fujii H, Miwa S. Expression and enzymatic characterization of human glucose phosphate isomerase (gpi) variants accounting for gpi deficiency. Blood Cells Mol Dis. 1998;24:54–61 [PubMed: 9616041]
47. Depre C, Shipley GL, Chen W, Han Q, Doenst T, Moore ML, Stepkowski S, Davies PJ, Taegtmeyer H. Unloaded heart in vivo replicates fetal gene expression of cardiac hypertrophy. Nat Med. 1998;4:1269–1275 [PubMed: 9809550]
48. Goodwin GW, Taegtmeyer H. Improved energy homeostasis of the heart in the metabolic state of exercise. Am J Physiol Heart Circ Physiol. 2000;279:H1490–1501 [PubMed: 11009433]
49. Goodwin GW, Arteaga JR, Taegtmeyer H. Glycogen turnover in the isolated working rat heart. J Biol Chem. 1995;270:9234–9240 [PubMed: 7721842]
50. Goodwin GW, Ahmad F, Taegtmeyer H. Preferential oxidation of glycogen in isolated working rat heart. J Clin Invest. 1996;97:1409–1416 [PubMed: 8617872]
51. DeBerardinis RJ, Mancuso A, Daikhin E, Nissim I, Yudkoff M, Wehrli S, Thompson CB. Beyond aerobic glycolysis: Transformed cells can engage in glutamine metabolism that exceeds the requirement for protein and nucleotide synthesis. Proc Natl Acad Sci U S A. 2007;104:19345–19350 [PubMed: 18032601]
52. Nakano H, Minami I, Braas D, Pappoe H, Wu X, Sagadevan A, Vergnes L, Fu K, Morselli M, Dunham C, Ding X, Stieg AZ, Gimzewski JK, Pellegrini M, Clark PM, Reue K, Lusis AJ, Ribalet B, Kurdistani SK, Christofk H, Nakatsuji N, Nakano A. Glucose inhibits cardiac muscle maturation through nucleotide biosynthesis. Elife. 2017;6
53. Düvel K, Yecies JL, Menon S, Raman P, Lipovsky AI, Souza AL, Triantafellow E, Ma Q, Gorski R, Cleaver S, Vander Heiden MG, MacKeigan JP, Finan PM, Clish CB, Murphy LO, Manning BD. Activation of a metabolic gene regulatory network downstream of mtor complex 1. Mol Cell. 2010;39:171–183 [PubMed: 20670887]
54. Porstmann T, Santos CR, Griffiths B, Cully M, Wu M, Leevers S, Griffiths JR, Chung YL, Schulze A. Srebp activity is regulated by mtorc1 and contributes to akt-dependent cell growth. Cell Metab. 2008;8:224–236 [PubMed: 18762023]
55. Eid AA, Ford BM, Bhandary B, de Cassia Cavaglieri R, Block K, Barnes JL, Gorin Y, Choudhury GG, Abboud HE. Mammalian target of rapamycin regulates nox4-mediated podocyte depletion in diabetic renal injury. Diabetes. 2013;62:2935–2947 [PubMed: 23557706]

NOVELTY AND SIGNIFICANCE

What Is Known?

- Metabolic and structural remodeling of cardiomyocytes is a hallmark of heart failure
- Mismatch between glucose uptake and oxidation is associated with accumulation of glucose 6-phosphate and activation of the mammalian target of rapamycin (mTOR)

What New Information Does This Article Contribute?

- Metabolic control analysis reveals that phosphoglucose isomerase activity controls glucose 6-phosphate concentration in cardiomyocytes
- Inhibition of phosphoglucose isomerase results in increased mTOR activation and protein synthesis cardiomyocytes

Metabolic alterations precede structural remodeling in the heart. The utilization of glucose can be a metabolic limitation for cardiac protein synthesis and renewal in response to stress. How cardiomyocytes integrate these signals and adapt structurally to sustain cardiac function is still an unanswered question. We demonstrate that phosphoglucose isomerase inhibition promotes glucose 6-phosphate accumulation and supports protein synthesis in cardiomyocytes. Mathematical modeling shows that phosphoglucose isomerase inhibition decreases glycolytic flux and redirects glucose 6-phosphate into the pentose phosphate pathway. We demonstrate that this redirection, in turn, activates mTOR, and increases protein synthesis. In conclusion, carbon flux in the heart is redirected from glycolysis into the pentose phosphate pathway to support biosynthetic processes.

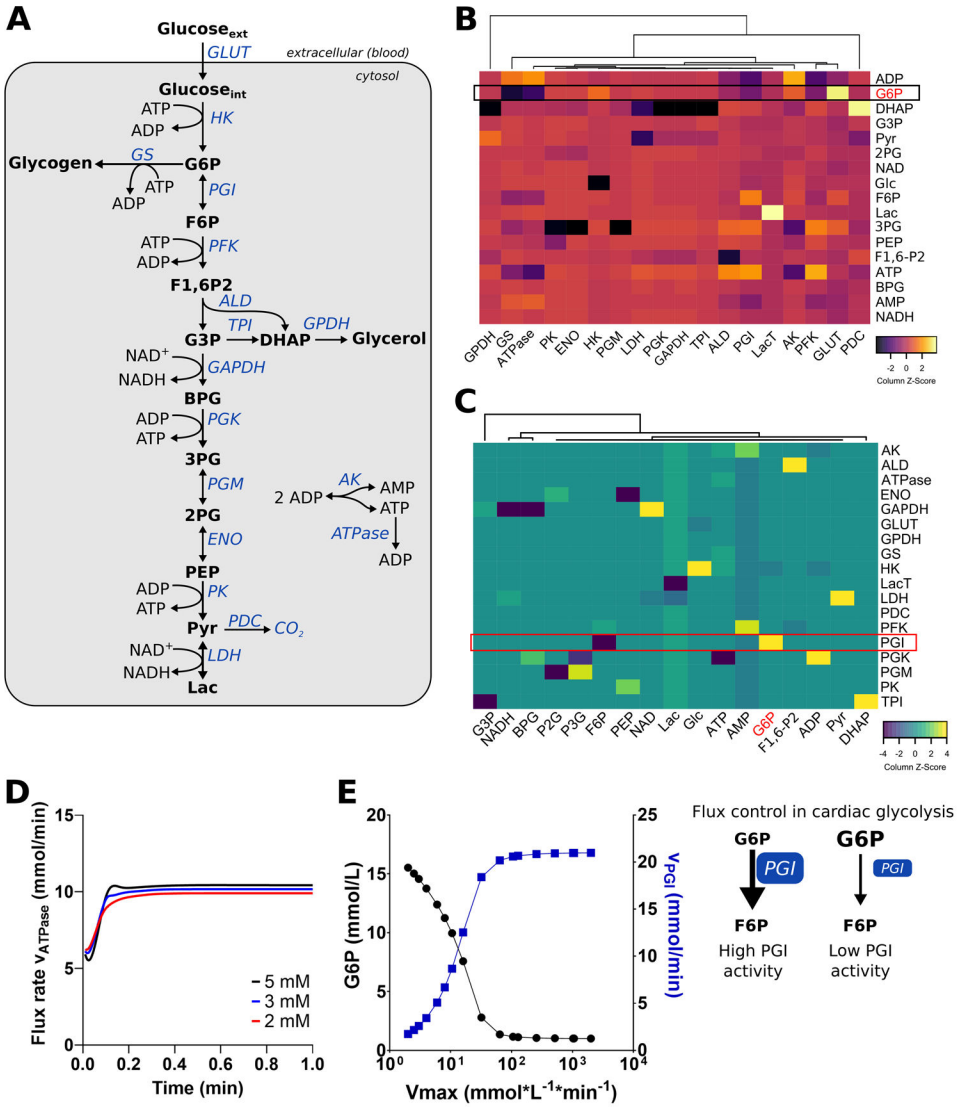

Figure 1. Metabolic control analysis of cardiac glycolysis using *CardioGlyco*.

(**A**) The metabolic model, *CardioGlyco*, is compartmentalized in extracellular space (blood) and cytosol. (**B-C**) Metabolic control analysis of cardiac glycolysis. Heat map of scaled estimated elasticities (**B**) and calculated control coefficients (**C**) using unsupervised hierarchical clustering. (**D**) Estimated flux rate of ATP hydrolysis (ATPase) as a function of time and at different glucose concentrations (2 to 5 mmol/L). (**E**) G6P concentration and flux through PGI as a function of the V_{max} of the PGI system. PGI V_{max} was varied, and G6P, as well as flux were calculated using *CardioGlyco*. Schematic depicting the rate-limiting effect of PGI. Abbreviations: AK, adenylate kinase; ALD, aldolase; BPG, bisphosphoglycerate; DHAP, dihydroxyacetone phosphate; ENO, enolase; F6P, fructose-6-phosphate; F1,6-P2, fructose 1,6-bisphosphate; Glc, glucose; GLUT, glucose transporter; G6P, glucose 6-phosphate; G3P, glycerol 3-phosphate; GAPDH, glyceraldehyde 3-phosphate dehydrogenase; GPDH, glycerol 3-phosphate dehydrogenase; GS, glycogen synthase; HK, hexokinase; Lac, lactate; LDH, lactate dehydrogenase; LacT, lactate transport; AK,

adenylate kinase; PGI, phosphoglucose isomerase; PFK, phosphofructokinase; PGK, 3-phosphoglycerate kinase; PGM, phosphoglucomutase; PK, pyruvate kinase; 3PG, 3-phosphoglycerate; 2PG, 2-phosphoglycerate; PEP, phosphoenolpyruvate; Pyr, pyruvate; PDC, pyruvate decarboxylase; TPI, triosephosphate isomerase.

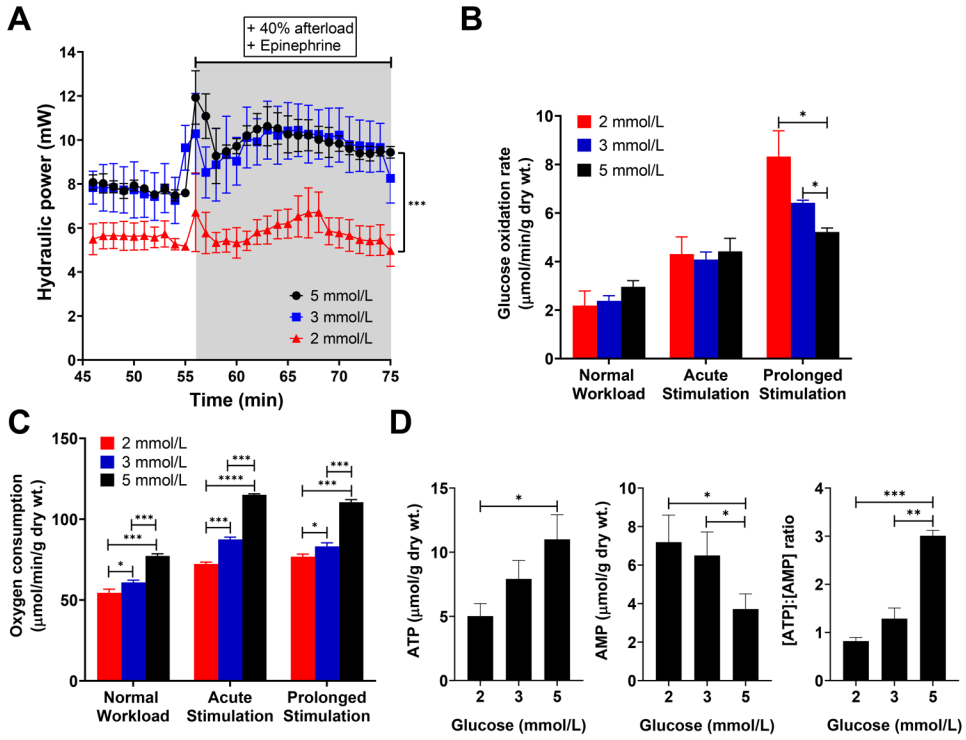

Figure 2. Cardiac performance in response to glucose deprivation.

(**A**-**C**) Hydraulic power (**A**), glucose oxidation rate (**B**), and myocardial oxygen consumption (**C**) at near-physiologic (100 cmH_2O, "Normal Workload", 45-55 min) and increased workload (140 cmH_2O, "Acute stimulation" 55-58 min, "Prolonged Stimulation" 65-75 min). n = 4 rats/ group. All data shown are mean ± s.e.m. Statistical analysis by Kruskal-Wallis test with post-hoc Dunn's multiple comparisons test. *P<0.05; **P<0.01; ***P<0.001. (**D**) ATP and AMP levels from perfused and then freeze-clamped rat hearts, and ATP to AMP ratio. Statistical analysis by one-way ANOVA with post-hoc Tukey's multiple comparisons test. n = 4 rats/ group. All data shown are mean ± s.e.m. *P<0.05; **P<0.01; ***P<0.001.

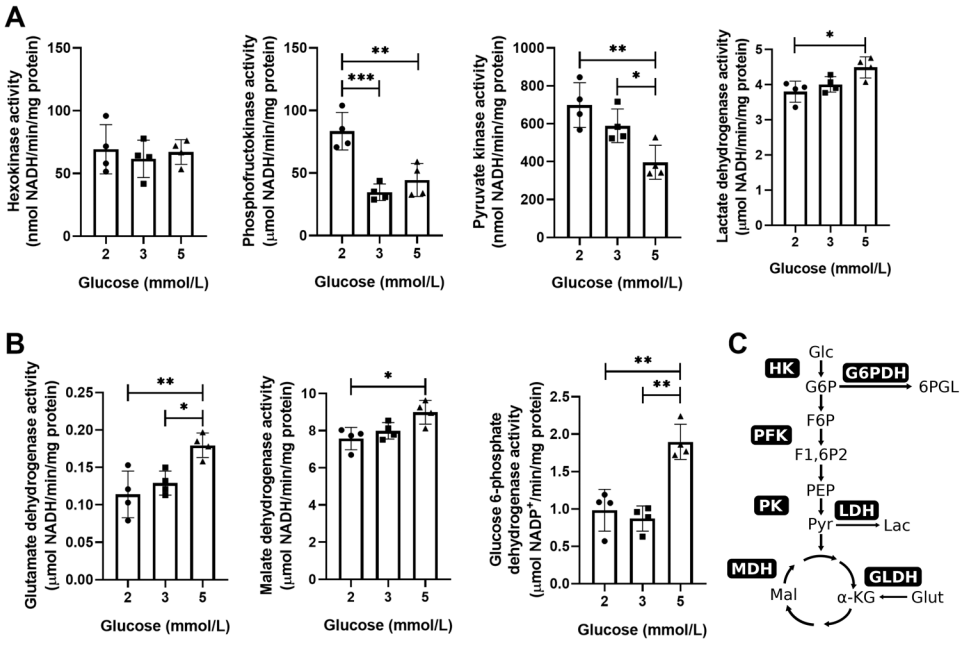

Figure 3. Enzymatic changes in response to glucose deprivation.

(**A**-**B**) Enzymatic activities of hexokinase (HK), phosphofructokinase (PFK), pyruvate kinase (PK), lactate dehydrogenase (LDH) (**A**), glutamate dehydrogenase (GLDH), malate dehydrogenase (MDH) and glucose 6-phosphate dehydrogenase (G6PDH) (**B**) from perfused and then freeze-clamped rat hearts. $n = 4$ rats/ group. All data shown are mean ± s.d.; Statistical analysis by one-way ANOVA and post-hoc Tukey's multiple comparisons test. *P<0.05; **P<0.01. (**C**) Schematic overview of measured enzymatic activities in relation to metabolic pathways. Enzyme activities were normalized to total tissue protein content. Abbreviations: Glc, glucose; G6P, glucose 6-phosphate; 6PGL, 6-phospho-D-glucono-1,5-lactone; Glut, glutamate; Lac, lactate; α-KG, α-ketoglutarate; Mal, malate; PEP, phosphoenolpyruvate; Pyr, pyruvate.

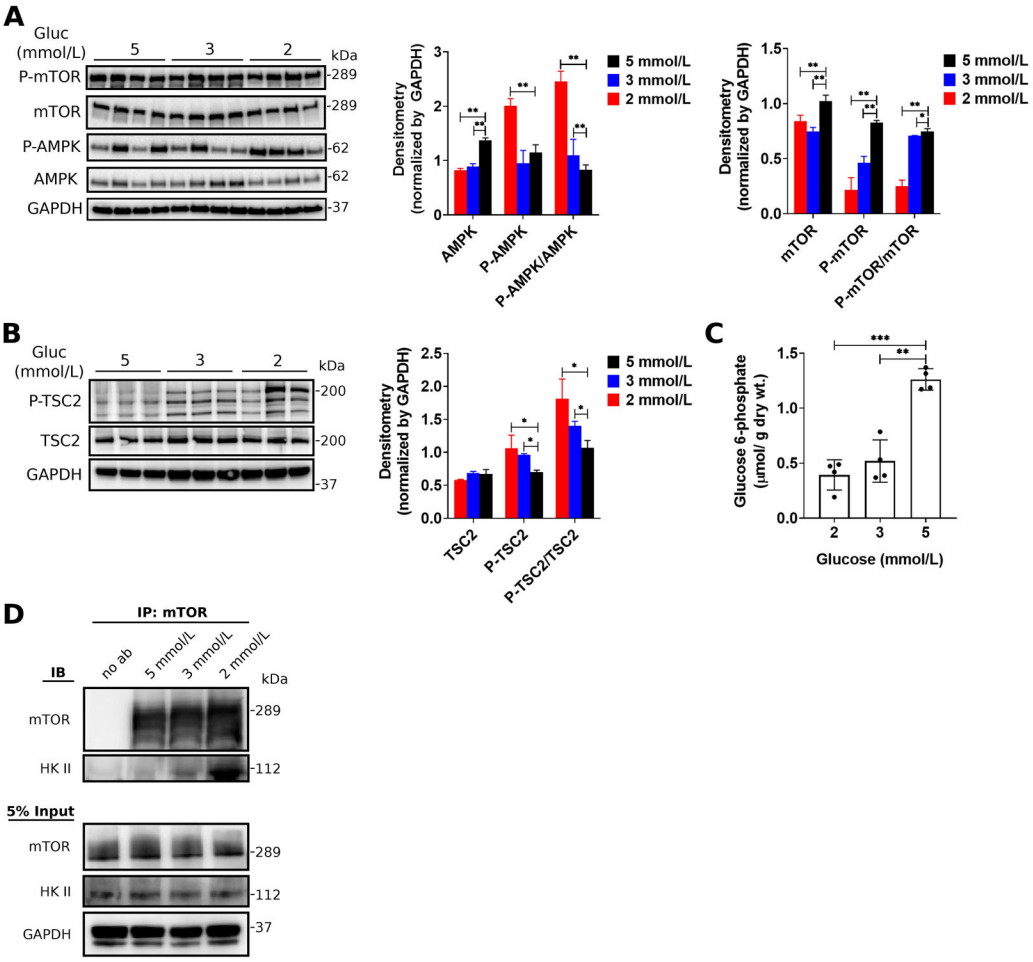

Figure 4. The role of glucose 6-phosphate and Hexokinase-II on the regulation of mTOR activity in response to glucose deprivation.

(**A**-**B**) Representative western blots and quantitative analysis of total protein expression and phosphorylation for AMPK and mTOR (**A**) as well as TSC2 (**B**) in response to glucose supply in isolated working adult rat hearts. The levels of protein expression were normalized to GAPDH on each gel. $n = 4$ rats/ group. All data shown are mean ± s.e.m. Statistical analysis by one-way ANOVA with Tukey's multiple comparisons test. *P<0.05; **P<0.01; ***P<0.001. (**C**) Glucose 6-phosphate (G6P) concentration in adult rat hearts perfused at physiologic (5 mmol/L) and sub-physiologic glucose concentrations (2 and 3 mmol/L). All data shown are mean ± s.e.m. Statistical analysis by one-way ANOVA with Tukey's multiple comparisons test. *P<0.05; **P<0.01; ***P<0.001. (**D**) Glucose deprivation increases the association between hexokinase II (HKII) and mTOR.

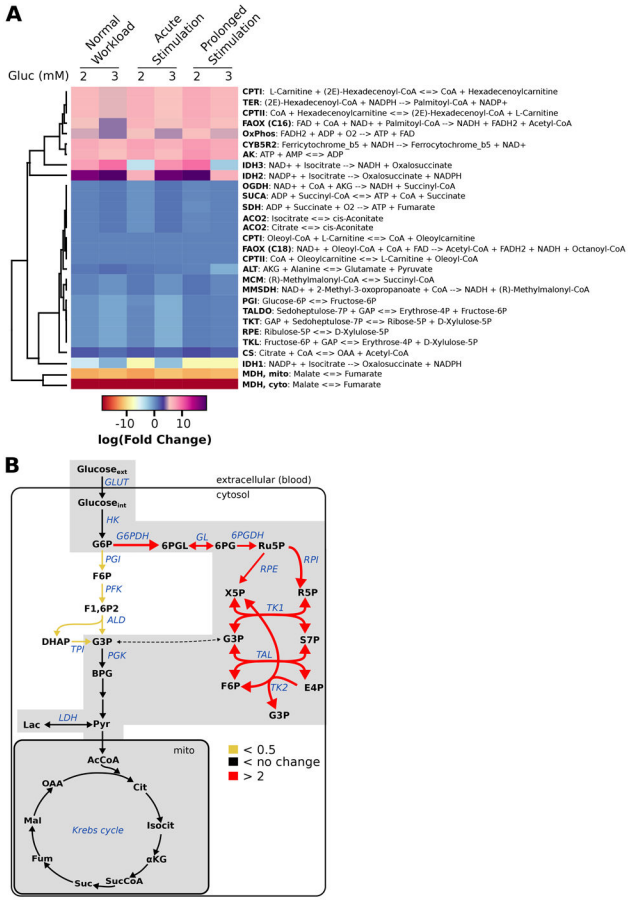

Figure 5. *CardioNet*-based simulation of phosphoglucose isomerase perturbations.

(**A**) Heat map of flux rate fold changes for enzymes and processes found to be increased or decreased by glucose deprivation (one-way ANOVA with Tukey's multiple comparisons test, $P<0.05$). Unsupervised hierarchical clustering reveals four main clusters with differential flux rates for (1) fatty acid oxidation and oxidative phosphorylation, (2) glycolysis and Krebs cycle, (3) isocitrate dehydrogenase 1, and (4) malate dehydrogenase. Flux rates were log10 transformed to normalize across different metabolic reactions. Flux distributions were calculated by Flux balance analysis (FBA) using the mammalian network of cardiac metabolism, *CardioNet*. Color scale indicates the degree to which flux rates are predicted to be respectively lower or higher in hearts perfused with 2 mmol/L or 3 mmol/L glucose relative to hearts perfused with 5 mmol/L glucose. (**B**) Schematic of *in silico* flux rate analysis for glucose metabolism in response to PGI inhibition. Edge thickness and color indicate the degree to which flux rates are estimated to be respectively lower or higher in response to phosphoglucose isomerase (PGI) inhibition. Abbreviations: AK, adenylate kinase; ACO2, aconitase; ALT, alanine aminotransferase; CS, citrate synthase; CPTI, carnitine palmitoyltransferase I; CPTII, carnitine palmitoyltransferase II; FAOX(C16), fatty acid oxidation of palmitate; FAOX(C18), fatty acid oxidation of oleate; OxPhos, oxidative phosphorylation; CYB5R2, cytochrome b5 reductase 2; IDH1, Isocitrate dehydrogenase 1; IDH2, Isocitrate dehydrogenase 2; IDH3, Isocitrate dehydrogenase 3; MCM, mehylmalonyl-CoA mutase; MDH, malate dehydrogenase; PGI, phosphoglucose isomerase; OGDH, α-

ketoglutarate dehydrogenase; RPE, Ribulose-phosphate 3-epimerase; SUCA, succinyl-CoA synthetase; SDH, Succinate dehydrogenase; TALDO, transketoaldolase; TKL, transketolase; TAL, transaldolase.

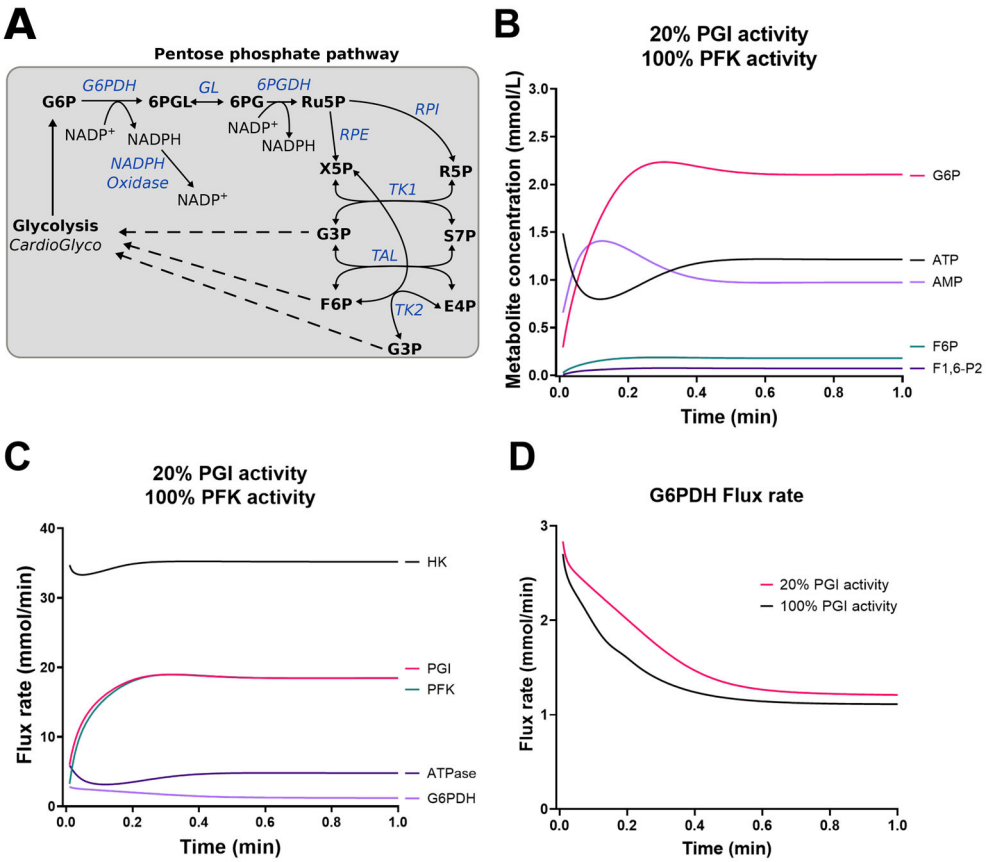

Figure 6. Kinetic modeling of phosphoglucose isomerase inhibition reveals redirection of glycolytic intermediates into the pentose phosphate pathway.

(**A**) Pentose phosphate pathway expansion of *CardioGlyco*. (**B**-**C**) Predicted metabolite concentrations (**B**) and flux rates (**C**) in response to PGI inhibition (20% activity). PFK activity was not changed. Extracellular glucose supply was set to 5.5 mmol/L during the simulations. (**D**) Comparison of G6PDH flux rate at 20% and 100% PGI activity. Simulations indicated that PGI inhibition promotes G6P accumulation and an increased G6PDH flux rate.

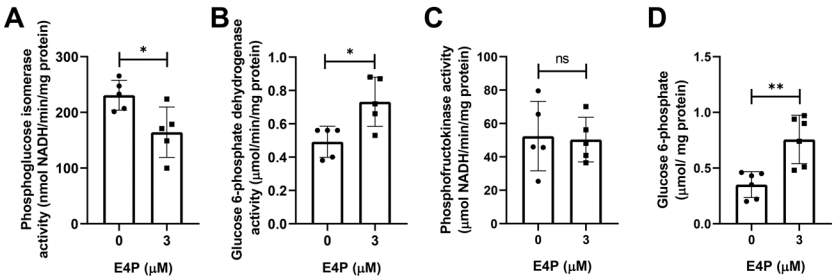

Figure 7. Phosphoglucose isomerase inhibition increases glucose 6-phosphate concentration and glucose 6-phosphate dehydrogenase activity.

Isolated adult mouse ventricular cardiomyocytes (AMVMs) were treated for 24 h with or without the phosphoglucose isomerase (PGI) inhibitor erythrose-4-phosphate (E4P, 3 μmol/L). (**A**-**B**) Treatment with E4P decreases PGI activity (**A**), which leads to an increased glucose 6-phosphate dehydrogenase activity (**B**). Phosphofructokinase activity showed no changes (**C**) *in vitro*. (**D**) Glucose 6-phosphate concentration increases in response to PGI inhibition by E4P in AMVMs. (**A**-**D**) n = 5 - 6 separate experiments/ group. Enzyme activities were normalized by total protein content from cell lysates. All data shown are mean ± s.d. Statistical analysis by unpaired t-test with Welch's correction. *P<0.05; **P<0.01; ***P<0.001; ns, not significant.

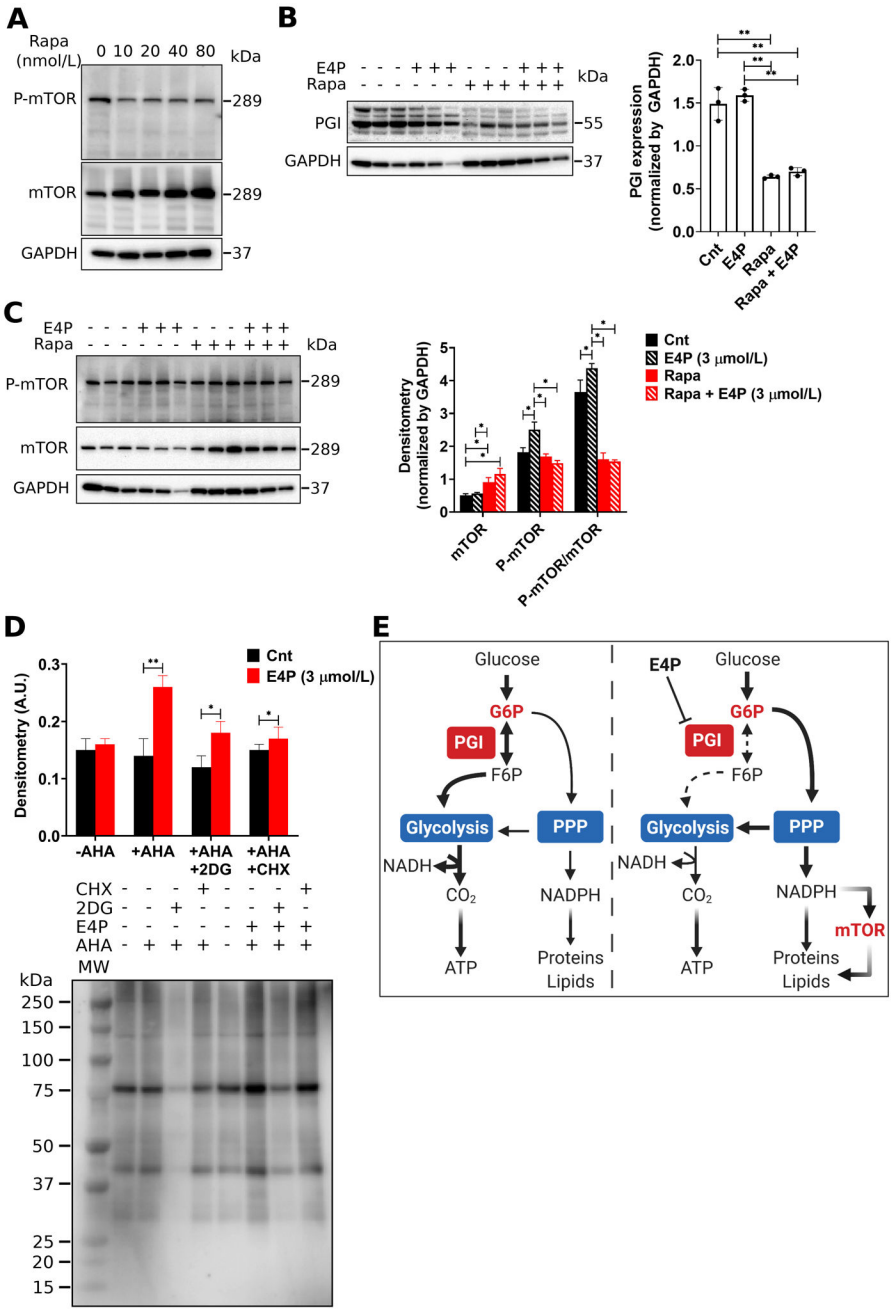

Figure 8. Phosphoglucose isomerase activity regulates glucose 6-phosphate concentration and mTOR activation.

(**A**) mTOR phosphorylation and activation in response to different rapamycin (Rapa) concentrations (0 to 80 nmol/L) in adult mouse ventricular cardiomyocytes (AMVMs). (**B**) Phosphoglucose isomerase (PGI) expression in response to phosphate-buffered saline (PBS), erythrose 4-phosphate (E4P; 3 µmol/L) or Rapa (20 nmol/L). E4P-mediated PGI inhibition does not affect total protein expression, while Rapa promotes the reduction of PGI expression. $n = 3$ independent experiments/ group. Data shown are mean ± s.d.; statistical analysis by one-way ANOVA and post-hoc Tukey's multiple comparisons test. $^{**}P<0.01$.

(**C**) mTOR phosphorylation in response to vehicle (PBS), E4P (3 μmol/L), or Rapa (20 nmol/L). $n = 3$ independent experiments/ group. Data shown are mean ± s.e.m.; statistical analysis by one-way ANOVA and post-hoc Tukey's multiple comparisons test. *$P<0.05$. (**D**) L-azidohomoalanine (AHA) labeling of newly synthesized proteins in AMVMs treated for 24 h with or without E4P or in response to 2-deoxyglucose (2DG, 25 mmol/L) and cycloheximide (CHX, 20 μmol/L). Representative western blot image of four independent experiments. Statistical analysis by one-way ANOVA and post-hoc Tukey's multiple comparisons test. *$P<0.05$; **$P<0.01$. (**E**) Schematic summarizing how PGI promotes redirection of flux into the pentose phosphate pathway (PPP). Schematic was created with Biorender.com. Abbreviations: ATP, adenosine triphosphate; G6P, glucose 6-phosphate; F6P, fructose 6-phosphate; NADH, nicotinamide adenine dinucleotide reduced; NADPH, nicotinamide adenine dinucleotide phosphate reduced.